Review

Author for correspondence:
Christopher S. Bretherton
e-mail: breth@washington.edu

Insights into low-latitude cloud feedbacks from high-resolution models

Christopher S. Bretherton

Department of Atmospheric Sciences, University of Washington, Seattle, WA 98195-1640, USA

Cloud feedbacks are a leading source of uncertainty in the climate sensitivity simulated by global climate models (GCMs). Low-latitude boundary-layer and cumulus cloud regimes are particularly problematic, because they are sustained by tight interactions between clouds and unresolved turbulent circulations. Turbulence-resolving models better simulate such cloud regimes and support the GCM consensus that they contribute to positive global cloud feedbacks. Large-eddy simulations using sub-100 m grid spacings over small computational domains elucidate marine boundary-layer cloud response to greenhouse warming. Four observationally supported mechanisms contribute: 'thermodynamic' cloudiness reduction from warming of the atmosphere–ocean column, 'radiative' cloudiness reduction from CO_2- and H_2O-induced increase in atmospheric emissivity aloft, 'stability-induced' cloud increase from increased lower tropospheric stratification, and 'dynamical' cloudiness increase from reduced subsidence. The cloudiness reduction mechanisms typically dominate, giving positive shortwave cloud feedback. Cloud-resolving models with horizontal grid spacings of a few kilometres illuminate how cumulonimbus cloud systems affect climate feedbacks. Limited-area simulations and superparameterized GCMs show upward shift and slight reduction of cloud cover in a warmer climate, implying positive cloud feedbacks. A global cloud-resolving model suggests tropical cirrus increases in a warmer climate, producing positive longwave cloud feedback, but results are sensitive to subgrid turbulence and ice microphysics schemes.

1. Introduction

For decades, estimates of the equilibrium climate sensitivity (ECS) to doubling of CO_2 simulated by global

climate models (GCMs) have had a large intermodel spread, with a 5th–95th percentile range of approximately 2–4.5 K [1,2]. Global cloud feedbacks are the largest contributor to this spread [2,3]. Fig. 7.10 from the Intergovernmental Panel on Climate Change (IPCC) Fifth Assessment Report (AR5) [2] showed global cloud feedbacks diagnosed from over 20 GCMs participating in recent rounds of the Coupled Model Intercomparison Project (CMIP3 and CMIP5) and Cloud Feedbacks Model Intercomparison Project (CFMIP2). These have an interquartile range of 0.5–0.9 W m^{-2} K^{-1}, and an overall intermodel spread of 0.2–1.4 W m^{-2} K^{-1}, including the effects both of warming and of rapid adjustments to increased CO_2. Given the CMIP3/5 multi-model mean Planck feedback (-3.2 W m^{-2} K^{-1}), water vapour/lapse rate feedback (1.0 W m^{-2} K^{-1}) and snow/ice albedo feedback (0.3 W m^{-2} K^{-1}), together with the radiative forcing of CO_2 doubling (3.7 W m^{-2} K^{-1}), all of which are fairly robustly known ([2], table 9.5), zero cloud feedback corresponds approximately to a 2 K ECS. Thus, if the GCM consensus of positive global cloud feedback is trustworthy, it places an important lower bound on ECS.

Much of the uncertainty in GCM-simulated cloud feedbacks derives from the formulation and interaction of GCM parametrizations for the processes that affect boundary-layer cloud, which are driven by turbulent circulations and associated subgrid variability not resolved in current GCMs. Parametrizations of these processes have become more sophisticated, incorporating ever more interaction between clouds and controlling factors such as thermodynamic, wind and radiative profiles, surface type and fluxes and aerosols ([2], ch. 7.2). In addition, GCM vertical and horizontal resolution has increased. This has presumably reduced the likelihood of surprise due to poorly represented physics, but it has not substantially reduced the overall uncertainty range. In 1989, Cess et al. [4] presented the first comprehensive atmospheric GCM (AGCM) intercomparison of cloud radiative response to a specified climate change (uniform 2 K sea-surface temperature (SST) increase). They found that the associated change in net global cloud radiative effect, or 'CRE feedback', ranged between -0.7 and 1.3 W m^{-2} K^{-1} across 14 participating models (note that global cloud feedback is approximately 0.7 W m^{-2} K^{-1} larger than CRE feedback [5]). In a 2014 study [6] of 12 CMIP5 GCMs subject to a 4 K SST increase, the intermodel spread of CRE feedback is only slightly smaller, -0.3 to 1.0 W m^{-2} K^{-1}, while typical AGCM horizontal grid spacings decreased from 300–750 km in [4] to 100–250 km in CMIP5. At regional scales, interaction with changing large-scale circulations and land-surface feedbacks can further increase uncertainty in the cloud response to climate change [7].

Observational 'emergent constraints' that relate cloud properties in the current climate to future climate sensitivity are one important strategy to reduce global cloud feedback uncertainty. This is an active area of research, and some promising constraints have been proposed. Qu et al. [8] showed that, in GCMs, the sensitivity of long-term climate trends in subtropical stratocumulus cloud cover to changes in temperature and lower tropospheric stability is similar to the corresponding sensitivity of these clouds to interannual variability, which has been accurately observed for 30 years. Sherwood et al. [9] found strong correlations between intermodel difference in climate sensitivity and their predictions of two complementary and observable indicators of how strongly cumulus clouds over the warmest parts of the tropical oceans exchange air with their environment. Both of these studies suggest that cloud feedbacks are at the high end of the GCM-predicted range. However, each of them has inevitable shortcomings, because the present is an imperfect analogy for the path to the future. Qu et al. used a single variable, estimated inversion strength (EIS), as a proxy for all sources of stratocumulus cloud variability that are not forced by a quasi-uniform warming of the entire ocean-lower-atmospheric column. Sherwood et al. relied on indicators from the deep tropics, yet the intermodel variability in global cloud feedbacks derives mainly from the subtropics. The study appealed to remote forcing through the Hadley circulation to connect the indicators to the cloud response, but no mechanistic evidence for this was given. To judge the robustness of these proposed emergent constraints is challenging, and relies on a good process-level understanding of how similarly clouds should respond to future climate change versus the range of conditions observed in the current climate. Because GCM parametrizations produce diverse predictions about cloud feedbacks, they cannot be expected to provide this process-level understanding. For that we turn to higher resolution

models that explicitly capture the cloud–turbulence interactions and cloud heterogeneity that are so challenging to parametrize.

To explicitly simulate boundary-layer and cumulus cloud formation processes requires a horizontal resolution of tens to hundreds of metres and a vertical resolution of the order of 10 m or less in the lower troposphere. For a multi-year global simulation, this is likely to remain computationally infeasible for decades hence. However, in the last decade various intermediate steps have been taken that shed light on what higher resolution simulations might teach us about cloud feedbacks, and how these predictions can be compared with observations.

In §2, we discuss one such step, small-domain large-eddy simulations (LESs) of the response of marine boundary-layer clouds to specified changes in their large-scale environment that are expected to accompany greenhouse warming. LESs have resolutions of 5–50 m in the vertical and 20–250 m in the horizontal over domains of a few kilometres on a side. In §3, we turn to cloud-resolving model (CRM) simulations of the response of deep convective cloud systems to greenhouse warming, using horizontal grid spacings of a few kilometres and tens of vertical levels. Some studies have used limited area domains of 100 or more kilometres on a side, and some span larger domains, including 'mock-Walker' simulations that span a range of SSTs inside the domain, 'superparametrized' simulations that include a small CRM within each grid column of a GCM in place of conventional physical parametrizations for moist turbulent processes, and a global CRM with resolutions as fine as 7 km.

These high-resolution models have led to a range of predictions about cloud feedback, but overall they support the GCM consensus that cloud feedbacks are likely to be positive and they have begun to provide a clearer understanding of several competing mechanisms of cloud feedback. Indeed, improved process-level understanding of cloud feedbacks was a primary reason that the AR5 assessed that 'the net radiative feedback due to all cloud types is likely positive' ([2], SPM D.1).

2. Large-eddy simulation of subtropical boundary-layer cloud feedbacks

LES is our most realistic modelling tool for cloud-topped boundary layers, because it resolves the turbulent eddies responsible for cloud formation and most of the vertical transports of heat, moisture and momentum. In an LES, cloud microphysical processes such as droplet formation, growth, precipitation and evaporation, the effects of subgrid turbulent eddies, radiative and surface turbulent fluxes must still be parametrized, but, unlike in a GCM, these parametrizations do not need to include a complex representation of subgrid variability, because most of this variability is resolved by the grid.

Model intercomparison studies suggest that current LESs robustly simulate some boundary-layer cloud types such as non-precipitating shallow cumulus, with little sensitivity of statistics such as cloud fraction or liquid water path to model details at easily achieved grid resolutions of 40 m in the vertical and 100 m in the horizontal [10]. LESs agree less well with each other and with observations for (i) stratocumulus under strong, sharp temperature inversions [11,12] and (ii) when precipitation formation is significant [13,14]. At a sharp inversion, fine vertical resolution is needed to simulate the inversion structure and its horizontal variability, and to resolve the small vertical eddies and filamentary downdrafts that mix the overlying air down into a stratocumulus layer. The strong longwave cooling of air at the cloud top reinforces the inversion strength and sharpness. Even with a vertical grid as fine as 5 m, many LESs tend to 'over-entrain', resulting in too thin a stratocumulus layer; this problem is exacerbated with coarser vertical resolution and is sensitive to the choices of advection scheme, subgrid turbulence parametrization, horizontal grid resolution, and even the very slight fall speed of cloud droplets.

Numerous field studies and satellite observations have shown that light precipitation is common in marine boundary-layer clouds of all types. This has led to advanced microphysical parametrizations in LESs predicting multiple moments of the size distribution of cloud and rain drops [15], or even discrete bin-resolved representations of that distribution [16]. In addition, interest in aerosol–cloud interaction and the aerosol indirect effect on climate has led many

LESs to include nucleation of cloud droplets from aerosol particles. While these processes are fundamentally well understood, diverse choices have been made in how to simplify them to be tractable for LESs, and these choices impact the simulated relationship between rain rate and cloud properties [13,14].

Despite these caveats, in a recent model intercomparison [17] based on an observed case of an airmass transitioning over 36 h from drizzling stratocumulus cloud to broken cumulus cloud as it moves over warmer water, the five participating LESs all showed remarkable skill in simulating the evolution of vertical thermodynamic structure, cloud thickness and fraction, precipitation rate and turbulence statistics. This suggests LESs can simulate quantitatively realistic cloud responses to large-scale change. In addition, an LES intercomparison of how boundary-layer clouds ranging from precipitating cumulus to non-precipitating stratocumulus respond to non-aerosol-related climate change [18] suggested that at least the sign of the simulated response in cloud fraction and thickness is consistent between LES models.

The application of LESs to predict marine boundary-layer cloud responses to climate change started in the last decade, as the models became more realistic and the computer power to run them for multi-day cases needed for such analysis became easily affordable. Blossey *et al.* [19], Xu *et al.* [20] and Rieck *et al.* [21] all compared LESs forced by conditions representative of a control and a perturbed, warmer climate and run out for a time long enough to assess the cloud response. Each study used a different model and a sufficiently different set-up (e.g. how much the free troposphere is warmed relative to the surface, whether subsidence or horizontal advective forcings are changed, etc.) that it is hard to compare the results, which included predictions both of low cloud decrease and of increase in a warmer climate.

(a) Findings from CGILS and related work

This motivated an LES intercomparison [18], carried out as part of the CFMIP-GASS Intercomparison of LES and SCMs (CGILS; [22]), to test whether different LESs, if given the same control climate and perturbation, would produce a similar cloud response. This was envisioned as providing a benchmark for testing cloud feedbacks simulated by single-column versions of climate models (SCMs). Summertime-mean forcings were specified for three northeast Pacific locations with different typical cloud regimes (shallow stratocumulus, decoupled stratocumulus and trade cumulus). After the surface flux and radiation parametrizations were carefully standardized across the LESs, they all produced fairly similar and realistic steady-state cloud-topped boundary layers, with little or no precipitation in the stratocumulus cases but precipitation playing an important role in the boundary-layer and cloud structure in the trade cumulus boundary layer. Each model was subject to the same idealized climate perturbation consisting of a 2 K warming of SST, which was moist-adiabatically enhanced in the free troposphere consistent with GCM simulations, and a 10% reduction in subsidence due to weakening of the tropical Hadley–Walker circulation. When just the warming but not the subsidence change was applied, every LES thinned the clouds with little change in boundary-layer depth (a 'thermodynamic' response). When subsidence was decreased, the LES deepened the boundary layer, allowing a 'dynamic' response in which the clouds thickened, counteracting the temperature-induced thinning to an extent that depended on the model. As a result, the net cloud change was not consistent between the LESs, but this was due to compensation between two cloud responses (thermodynamic and dynamic) that were consistent between models. This helps rationalize why quantitative simulation of low cloud response to climate change is even more difficult for GCMs, in which diverse parametrization assumptions can strongly affect the compensating thermodynamic and dynamic cloud responses.

Bretherton *et al.* [23] explored the role of many more environmental changes expected to accompany global warming, including changes in inversion strength, free-tropospheric humidity, wind speed and CO_2 on the CGILS cases, using a single LES. They also developed a composite case (dCMIP3) in which all of these forcings were combined following best estimates from GCMs. One key finding was that there was reduced low cloud in the dCMIP3 case for all three CGILS
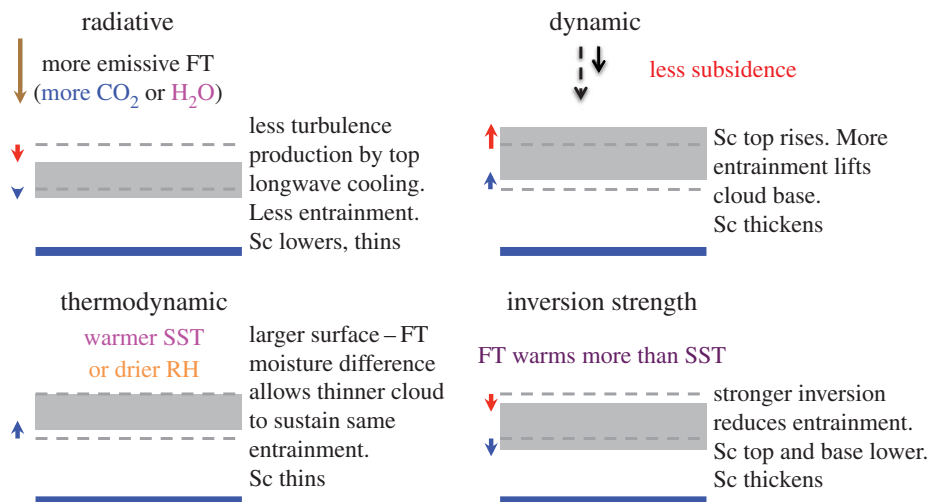
5

rsta.royalsocietypublishing.org *Phil. Trans. R. Soc. A* 373: 20140415

Figure 1. Marine boundary-layer stratocumulus cloud feedback mechanisms. In the figure, Sc denotes stratocumulus, RH denotes relative humidity, and FT denotes the free troposphere. Adapted from [23]. (Online version in colour.)

cloud regimes; this finding has since been replicated by several other LESs in a CGILS follow-on intercomparison (PN Blossey 2015, personal communication). Bretherton *et al.* categorized four types of low cloud response, illustrated in figure 1 and listed in decreasing order of importance given the dCMIP3 climate perturbation. These apply primarily to stratocumulus cloud layers, with a large cloud fraction, a distinct capping inversion, with or without underlying cumulus clouds, but the CGILS trade cumulus results [18,23] suggest that modified versions of these response mechanisms also apply to shallow cumulus clouds. For stratocumulus with nearly 100% cloud cover, they operate primarily by changing the horizontal-mean cloud thickness and liquid water path, and hence its optical depth. In broken cloud regimes such as the CGILS trade cumulus case, the response in cloud fraction tends to drive the response in radiative fluxes [18,23].

(i) Stratocumulus cloud reduction mechanisms

Thermodynamic: larger inversion specific humidity gradient (due to warmer climate or drier free troposphere) promotes more efficient turbulent entrainment-driven drying of the boundary layer. Several arguments of varying rigour have been given for this. Bretherton & Blossey [24] provided an explanation for thermodynamic stratocumulus reduction in terms of Clausius–Clapeyron 'entrainment liquid-flux feedback' driven by stronger humidity and liquid water fluxes in the cloud layer; see also [23]. Dussen *et al.* [25] performed idealized LESs with the same SST but different inversion temperature and humidity jumps. To each such case, they applied a uniform temperature increase with fixed relative humidity and simulated a cloud thinning, consistent with the thermodynamic mechanism. They suggested that the increased humidity jump is the primary control on the stratocumulus cloud thickness. Changes in wind speed or horizontal temperature advection also affect boundary-layer turbulence and cloud cover, and are likely to affect regional patterns of low cloud change, but appear to be of less importance for global cloud feedbacks [23]. *Radiative*: increased free-tropospheric greenhouse gases (CO_2 and water vapour) inhibit longwave radiative cooling from boundary-layer cloud tops, decreasing convective vertical moisture transport.

(ii) Stratocumulus cloud increase mechanisms

Stability: larger inversion temperature increase reduces dry air entrainment.
Dynamic: less subsidence allows a deeper inversion with more vertical development of clouds.

Bretherton & Blossey [24] confirmed these mechanisms (and their relative importance) in an LES of a composite stratocumulus to cumulus (Sc-Cu) transition subject to climate perturbations.

(b) Observational support for these stratocumulus cloud response mechanisms

An advantage of mechanistic explanations of low cloud response is that they may be compared with observations of other situations in which the mechanism should operate. All of the above mechanisms have qualitative observational support of this type. Quantitative comparisons are challenging because all the LES cases to date have been idealized in important ways, and because it is difficult to remove the effects of possible covarying confounding factors in estimated cloud responses to particular forcings. In this section, the mechanisms will be discussed in historical order, which largely reflects their importance for low cloud space–time variability in the current climate rather than for climate change. This allows a better appreciation for how mechanistic understanding of controls on low cloud has built up over recent decades.

(i) Stability mechanism

Stability-driven enhancement of cloud cover explains much of the observed geographical and seasonal variation of stratocumulus cloud observed by surface observers and satellites in the current climate [26,27]. EIS is a skillful climatological predictor of geographical and seasonal variations in marine stratocumulus cloud cover in the current climate across a substantial range of SSTs [27]. EIS is an attractive measure of stability for climate change purposes since it is designed to remove the expected moist-adiabatic stabilization of the free-tropospheric potential temperature profile in a warmer climate, hence it provides a somewhat climate-invariant estimate of the capping inversion strength [27]. The shortwave cloud radiative effect (SWCRE) of stratocumulus cloud is observed to become approximately $1 \, \text{W m}^{-2}$ more negative for each 1% cloud fraction increase ([26], fig. 3), while cloud fraction also increases 5–6% per K increase in EIS ([27], fig. 6; [28], table 2), implying an observed sensitivity $\partial \text{SWCRE}/\partial \text{EIS} \approx -5 \, \text{W m}^{-2} \, \text{K}^{-1}$. LESs of the three CGILS cases [23] gave $\partial \text{SWCRE}/\partial \text{EIS} = 0$ to $-5 \, \text{W m}^{-2} \, \text{K}^{-1}$ (based on P2SFT versus P2S cases from their figs 6, 12, 16, which differed only in having an EIS increase of approximately 2 K), while LESs of a composite Sc–Cu transition case [24] gave $\partial \text{SWCRE}/\partial \text{EIS} = -10$ to $-15 \, \text{W m}^{-2} \, \text{K}^{-1}$ (based on dEIS versus P4 cases in their table 2). These LES results do not encompass enough of the low cloud variability within the subtropics to make a close comparison meaningful, but at least they bracket the observations. LESs of a highly idealized stratocumulus layer with a very strong inversion showed the reverse result—thinning of the cloud layer with increased inversion strength [25], suggesting caution in using this case as a guide to the response of real stratocumulus to environmental factors and climate change.

(ii) Dynamical mechanism

Myers & Norris [29] presented observational evidence for the dynamic cloud response mechanism (weaker subsidence favours more cloud). They analysed satellite-derived monthly mean marine low cloud cover and liquid water path, considering both geographical and seasonal variations and also interannual variability of low cloud at a fixed location. As EIS is a strong control on low cloud variability, its impact must be controlled for when analysing the role of other cloud-controlling factors [28]. Hence, they binned their data by EIS and 700 hPa mean pressure velocity ω_{700}. For fixed EIS, they found that stronger mean subsidence (larger ω_{700}) is associated with less and thinner cloud, with a lower cloud top. These observed responses were estimated to be $-\partial \text{CF}/\partial \omega_{700} = 1 - 2$, $-\partial \text{LWP}/\partial \omega_{700} = 3 - 5$, $-\partial z_{\text{inv}}/\partial \omega_{700} = 50$, where the units of ω_{700} are $10 \, \text{hPa d}^{-1}$, cloud fraction (CF) is in per cent, liquid water path (LWP) is in g m^{-2}, and inversion height z_{inv} is in metres, all with relative uncertainties of 20–100%, and the ranges hold for both geographical variations and interannual variations [29]. The three CGILS LES cases S6, S11 and S12 gave ranges, respectively, of $-\partial \text{CF}/\partial \omega_{700} = 0$, $-\partial \text{LWP}/\partial \omega_{700} = 0 - 3$,

7

rsta.royalsocietypublishing.org *Phil. Trans. R. Soc. A* **373**: 20140415

and $-\partial z_{inv}/\partial \omega_{700} = 25 - 50$ in the same units, estimated from tables and figures in [18,23]. These LES ranges are again consistent with the observational estimates.

(iii) Thermodynamic mechanism

Qu *et al.* [8] gave observational support for the thermodynamic cloud response mechanism. They performed multiple regressions of the interannual variability of low cloud cover on SST and EIS in five subtropical stratocumulus regimes. They interpreted SST as a proxy of overall air–sea column temperature change and used EIS to control for stability-associated cloud changes. They found that, for fixed EIS, positive SST anomalies are associated with negative cloud cover anomalies, consistent with the thermodynamic mechanism. They also found that, in GCMs, the regression of simulated interannual variability of low cloud on EIS and SST in the stratocumulus regions was consistent with their simulated low cloud response to twenty-first-century climate change, in which there are small increases in EIS and large increases in SST. That is, their observational analysis suggests that low cloud will decrease as SST warms, consistent with the thermodynamic mechanism, and in fact the implied positive cloud feedback is at the upper end of GCM predictions for the stratocumulus regions.

Qu *et al.* did not control for subsidence, which may alias into their regression results. Bony & Dufresne [30] compared interannual cloud variability over the low-latitude oceans in GCMs with more versus less positive global cloud feedbacks. They used vertical velocity binning [7] to isolate the thermodynamic cloud response of GCMs to tropics-wide temperature. Like [8] they found that GCMs with stronger positive cloud feedbacks also show stronger interannual response of cloud to tropical warming.

Qu *et al.*'s table 6 predicts a 5% low cloud cover decrease for a 2 K SST warming. According to their fig. 2, this corresponds to a $-4\,\mathrm{W\,m}^{-2}$ SWCRE change, which is a 10% decrease from the climatological SWCRE in the stratocumulus regions [26]. The CGILS LESs also predict an approximately 10% decrease in SWCRE for a 2 K SST warming [18,23], albeit based on optical depth changes in a much thicker control cloud layer with 100% cloud cover, rather than cloud fraction changes. While the CGILS Sc cases are too idealized to justify a rigorous comparison, these two estimates of the thermodynamic sensitivity of low cloud are in the same range.

One concern with Qu *et al.*'s analysis is that the regression of cloud fraction on SST and EIS that works for decadal variability and climate change does not also explain the geographical and seasonal variation of low cloud cover, which is instead well explained by EIS alone across a 15 K range of SSTs [27]. This suggests that other environmental predictors play important roles in determining low cloud cover in at least one of these two contexts.

(iv) Radiative mechanism

Observational support for the radiative cloud reduction mechanism comes from a satellite-based study by Christensen *et al.* [31] of the effect of cirrus that advect over underlying stratocumulus. This study selects cases from CloudSat overpasses in which some stratocumulus is covered by thin non-precipitating cirrus, while adjacent stratocumulus is not obscured by cirrus. The cirrus, like a greenhouse gas, increases downwelling longwave radiation onto the stratocumulus. Christensen *et al.* found a statistically significant stratocumulus thinning and drizzle reduction under the cirrus, as expected from the radiative low cloud reduction mechanism. These data are not amenable to quantitative comparison with the CGILS results because the downwelling radiation changes due to the cirrus cannot reliably be inferred, and there is not enough time for the stratocumulus response to reach equilibrium. GCMs also tend to predict radiatively driven reduction in marine stratocumulus cloud, as shown from simulations in which CO_2 is abruptly quadrupled while either keeping SST fixed [28] or considering the rapid (days to weeks) adjustment of cloud in a coupled integration, before SST has time to respond [32].

8

rsta.royalsocietypublishing.org *Phil. Trans. R. Soc. A* **373**: 20140415

(c) Shallow cumulus response to climate change

The response of pure trade cumulus cloud to climate change is less clear. The forcing specification in the CGILS cases caused artificial overdeepening of the trade inversion ([18] Sec. 5.1.2), which was particularly pronounced for the shallow cumulus case. As a result the LESs simulated cumulus clouds 3–4 km deep, for which precipitation feedbacks reduce the cloud response to warming [18].

Rieck *et al.* [21] compared LESs of an idealized trade cumulus case in which the entire temperature profile was uniformly warmed by up to 8 K without changing the relative humidity. They found an increase in cumulus depth, drying of the boundary layer by the associated increase in penetrative entrainment and a slight decrease in cloud cover in a warmer climate. This study was similar in spirit to the CGILS cases, except the warming was not increased moist-adiabatically with height, so the EIS was reduced in a warmer climate, explaining the boundary-layer deepening on stability grounds alone. As with stratocumulus, wind speed reduction that might also accompany climate change reduces surface moisture flux and LES-simulated trade cumulus cloud cover, while shallowing the cumulus layer [21,33]. In contrast to stratocumulus regimes, trade cumulus boundary layers may experience stronger radiative driving in a warmer climate because of enhanced clear-sky cooling rates in the moister air between clouds [34].

In both LESs [10,35] and observations [36], there is a very persistent layer of nearly non-buoyant trade cumulus clouds just above the lifted condensation level of the subcloud mixed layer, at the base of the weakly stably stratified transition layer beneath the conditional unstable shallow cumulus layer. The transition layer is a gatekeeper. Its stratification dynamically adjusts the supply of moist subcloud updraft air to the overlying cumuli that feed off radiative destabilization [37]. The transition layer clouds are thus a mixture of nascent cumulus updrafts and 'failed' updrafts that are too weak to penetrate into the cumulus layer. Their combined cloud coverage (20% in Barbados observations) changes remarkably little in response to synoptic variability, instead reflecting tight feedback control due to its gatekeeper role [36]. Rieck *et al.* suggest this coverage might marginally decrease in a much warmer climate, but perhaps other factors may also be important to cloud feedbacks from trade cumulus regions. For instance, in the Caribbean area, low cloud cover is more strongly modulated by transient inversion cloud that might behave more like stratocumulus rather than the shallow cumulus cloud cover [36]. More study of this regime is needed.

That said, Rieck *et al.*'s explanation for the sensitivity of shallow cumulus cloud to warming is similar to the thermodynamic (entrainment liquid-flux feedback) mechanism for stratocumulus cloud reduction. The common ground is that, in a warmer climate, boundary-layer clouds of a given thickness generate turbulence and entrain dry air from above more efficiently, which feeds back to reduce the cloudiness.

(d) Synthesis

In the current climate, marine low clouds are most strongly regulated by inversion stability. For climate change, LESs suggest that the most important mechanisms of low cloud response are thermodynamically and radiatively driven cloud reduction, partly compensated by regionally varying increases in inversion stability and decreases in subsidence. All of these mechanisms have observational support. As a group, GCMs also tend to show thermodynamic (temperature-mediated) and radiative low cloud decrease (rapid adjustment at the onset of abrupt CO_2 quadrupling), leading to positive low cloud feedback on climate, but with large scatter in magnitude [38–40]. The most important mechanism for decreasing subtropical low cloud in a warmer climate is thermodynamic and is due to enhanced convective mixing efficiency—a given field of low clouds produces more upward liquid water flux and entrainment of dry free tropospheric air in a warmer climate, leading to drying of the boundary layer and cloud reduction.

In general, given adequate grid resolution, LESs and CRMs naturally simulate the cloud fields created by the interaction of moist turbulence and cumulus convection, because both are just

forms of eddying motion. On the other hand, in GCMs, different parametrizations handle cloud properties, turbulence and cumulus convection, and their subgrid interactions are enormously challenging to consistently and accurately simulate [41,42], contributing to the range of GCM-simulated tropical cloud feedback [22,43]. Appropriately designed GCM parametrizations should still support the same cloud response mechanisms isolated in LESs and observations, and an important ongoing challenge is the design of GCM diagnostics that quantitatively test this.

3. Cloud feedbacks simulated by cloud-resolving models

Most of the precipitation and much of the cloud in the tropics, and, seasonally, in parts of the midlatitudes, is due to deep convective cloud systems. The parametrization of deep convection and related cloud processes is a major uncertainty for GCMs, and their simulated global cloud feedbacks can be sensitive to cumulus parametrization. Stainforth *et al.* [44] showed using a perturbed parameter ensemble that the climate sensitivity of the HadAM3 model was highly dependent on a lateral entrainment coefficient in the cumulus parametrization. Gettelman *et al.* [45] compared the climate sensitivity of two versions of the NCAR-DOE Community Atmosphere Model (CAM4 and CAM5). The much larger climate sensitivity of CAM5 versus CAM4 was traced mainly to the use of a new shallow cumulus parametrization. Zhao [46] showed that the climate sensitivity of different versions of the Geophysical Fluid Dynamics Laboratory climate model were sensitive to the formulations of the lateral entrainment rate and precipitation formation in the updraft, because these formulations affected how cumulus cloud properties and precipitation efficiency depend on temperature. Webb *et al.* [47] show that removing cumulus parametrizations in a set of GCMs noticeably affected their global cloud feedbacks, though not necessarily in a particular direction.

(a) Radiative–convective equilibrium simulations by cloud-resolving models

Hence it is illuminating to also consider how deep convective clouds respond to climate perturbations in CRMs, in which larger convective updrafts and downdrafts are resolved by using horizontal grid spacings of a few kilometres and tens of vertical levels. As with LESs, these models are computationally intensive, so the problem must be idealized by using limited area domains, short simulations or both. As with LESs, microphysics and subgrid turbulence must still be parametrized. Ice and mixed-phase microphysics in deep convective clouds are much more complex and uncertain than the warm (liquid) cloud microphysics in subtropical boundary-layer clouds.

Limited-area CRM simulations of radiative–convective equilibrium (RCE) provided an early framework for looking at how deep convective cloud systems might respond to warming. A seminal study by Tompkins & Craig [48] examined RCE in a 60×60 km wide by 21 km deep domain with horizontally uniform SSTs of 298, 300 and 302 K, using 45 day simulations with 2 km horizontal grid spacing Δx and 35 variably spaced vertical grid levels. They found that the entire cloud distribution above 3 km altitude shifted upward following isotherms in a warmer climate, with a very slight reduction in horizontal extent (figure 2). Similar results were obtained by Kuang & Hartmann [49]. Hartmann & Larson [50] explained the upward cloud shift using a radiative mechanism, the 'fixed anvil temperature' (FAT) hypothesis. The idea underlying FAT is that the convective cirrus anvils mark the top of the tropospheric layer of efficient clear-sky radiative cooling, which has a fixed temperature since efficient radiative cooling requires that air be warm enough to hold significant water vapour. They also emphasized that FAT is a strong positive cloud feedback, because the infrared emission temperature of the cloud, and hence the overall longwave radiative energy loss, is reduced by the upward shift of the cloud compared with the no-feedback case of a cloud which stays at the same altitude. Zelinka & Hartmann [51] showed that a similar upward shift is robustly simulated by GCMs. The simplicity of FAT, and its robustness across model classes, contributed to the AR5 assessment that global cloud feedbacks are likely to be positive.
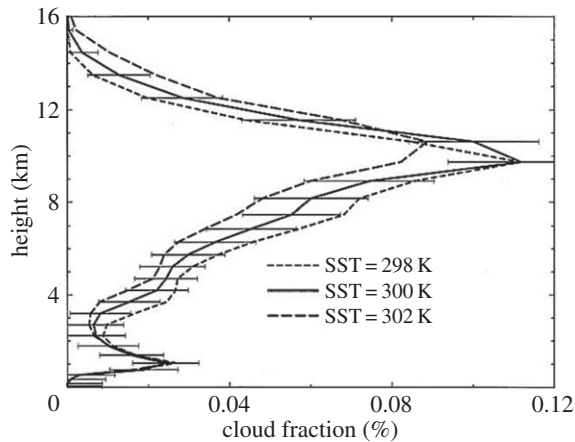
Figure 2. Cloud fraction in RCE simulation with three SSTs. Adapted from [48].

RCE simulations also tend to show a slight reduction in anvil cloud fraction with warming [48,49]. A slight reduction in cumulus updraft mass flux with warming ([48], fig. 8) may decrease upper-tropospheric detrainment into cirrus anvils. Because the anvils encompass cirrus clouds with a range of optical thickness, reduced anvil cloud causes roughly compensating positive shortwave and negative longwave cloud feedbacks [48]. This is in contrast to the hypothetical 'iris' effect [52] associated with reduction mainly of optically thin cirrus, for which the negative longwave cloud feedback would dominate.

Another interesting feature in figure 2 is the remarkable invariance of the cloud cover profile below 2 km altitude (the shallow cumulus population) to SST warming. This echoes the results noted earlier for trade cumulus, where LESs suggested only marginal reductions in cloud fraction with warming, in contrast to the much stronger positive cloud feedbacks simulated by LESs in stratocumulus regimes. As in that case, this low-level cloud cover maximizes near the shallow cumulus cloud base. RCE simulations of Kuang & Hartmann [49] also show this invariance, though their simulations show some cloud cover reduction between 2 and 4 km altitude in a warmer climate that is sensitive to the CRM microphysics parametrization and may reflect interactions with melting of precipitation from deep cumulus cloud systems.

(b) Global cloud-resolving simulations

A global cloud-resolving model (GCRM) is arguably the ideal modelling tool for studying deep convective cloud feedbacks, because it simulates the entire range of scales from the cumulus updrafts to global circulations. Despite its computational enormity, such a model exists and has been used to study cloud feedbacks. The Japanese NICAM model has been run with near cloud-resolving (7 km) horizontal resolution for 30 days and 14 km horizontal resolution for 90 days, with climatological SSTs and a uniform 2 K SST increase [53–55].

Tsushima *et al.* [55] investigated the sensitivity of this experiment to selected changes in the physics parametrization with 14 km resolution (figure 3). Such short simulations can robustly identify only very large cloud responses given natural variability. The 7 and 14 km standard-physics NICAM simulations in figure 3 greatly overestimate tropical cirrus cloud cover in the present climate and show very strong positive longwave cloud feedback due to even more tropical cirrus in a warmer climate. Surprisingly, this sensitivity was traced primarily to the formulation of subgrid vertical turbulent mixing, with a secondary contribution from the formulation of snow fall speed. They sought but did not find a simple explanation for these results. The NICAM experience emphasizes that, even within a GCRM, the physical parametrizations matter to the results. Reassuringly, the sensitivity study in which high cloud
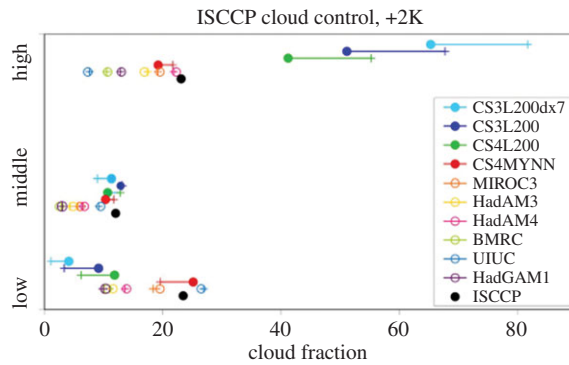
Figure 3. Tropical-mean (30S–30N) cloud fraction in four configurations of the NICAM global cloud-resolving model with control SSTs (filled circles) and with SST uniformly increased by 2 K (+). CS3L200dx7 and CS3L200 denote standard-physics simulations with 7 and 14 km horizontal resolution, respectively. Two 14 km perturbed-physics simulations are shown: CS4L200 has increased snow fall speed, and CS4MYNN also has a revised subgrid turbulent mixing scheme. The open circles are results from conventional GCMs, and the black circle is a satellite estimate. Adapted from [55]. (Online version in colour.)

cover in the present climate matches satellite observations (CS4MYNN in figure 3) also has much smaller cirrus cloud increases and less positive cloud feedback, in line with conventional GCMs.

(c) Results from superparametrization

Superparametrized climate models are intermediate between GCRMs and conventional GCMs. They employ the same horizontal grid as a GCM, but use a small CRM in place of the moist atmospheric physics parametrizations (cumulus convection, turbulent mixing, cloud processes) in each grid column of the GCM [56–58]. The computational expense of superparametrization is about 100 times that of a conventional GCM with the same resolution, but the model architecture is very efficiently parallelized, as the CRMs only need to communicate on the GCM time step, during which they have independently done a great deal of computation. A GCRM increases the needed computation by a further factor of 100 compared with superparametrization.

It is now possible to run superparametrization in the atmospheric component of fully coupled climate models [59,60], and in other CMIP/CFMIP style model intercomparisons that require decade to century long integrations [61]. In future, superparametrization may allow coupling of LESs with resolutions sufficiently fine to simulate boundary-layer cumulus and stratocumulus clouds into global climate models for climate-length simulations, a daunting challenge for GCRMs.

Cloud feedbacks have been explored in multiple versions of SPCAM, the superparametrized Community Atmosphere Model. Wyant *et al.* [34,62] studied the sensitivity of the first version, SPCAM3, to a uniform 2 K SST increase, finding negative shortwave cloud feedbacks at the bottom end of what had been simulated in CMIP-class models. These were due to low cloud increases over most of the subtropical oceans. Wyant *et al.* [63] analysed the response of a later version of SPCAM3 to CO_2 quadrupling with fixed SST, finding a shift of cloud from ocean to land but negligible globally averaged cloud changes. These studies used very short integrations of 2.5–3.5 years, inducing large sampling uncertainty, especially for sub-global-scale features. Bretherton *et al.* [61] analysed cloud feedbacks in a more recent version, SPCAM4, in which the dynamical core of the host climate model was changed from spectral to finite-volume. A CMIP5-style 150 year abrupt CO_2 quadrupling experiment including dynamical ocean coupling (a configuration called SPCCSM4) was supplemented by 35 year $4 \times CO_2$ fixed SST and 4 K uniform SST warming experiments. Overall, SPCCSM4 net cloud feedbacks (figure 4) were within the mid-range of conventional GCMs participating in CMIP3/CMIP5, including high-latitude cloud increases and mid-level cloud decreases. SPCCSM4 exhibited unusually large low cloud decreases over land

due to both warming and CO_2 increase, driven by decreased surface water availability and relative humidity. This compensated for a slight low cloud increase over the oceans, smaller than seen in SPCAM3, to produce a global mean net cloud feedback of $0.49\,W\,m^{-2}\,K^{-1}$ similar to the CMIP5 multi-model mean These regional patterns were different from those in the conventionally parametrized version of CCSM4, which showed large Southern Ocean cloud decreases and more muted low cloud decreases over land, even though the global cloud feedbacks were not that different [61]. A version of SPCAM4 to which a sophisticated higher order closure scheme for representing subgrid cloud and turbulence has been added shows different patterns of regional cloud change from SPCAM4 when subjected to a 2 K SST increase (A Cheng 2015, personal communication). Unlike in NICAM, no version of SPCAM exhibits significant tropical cirrus cloud increases in a warmer climate. The sensitivity of low cloud feedbacks in superparametrized GCMs to details of model formulation, even when just considering the low-latitude oceans and a uniform SST increase, is disappointing. It reinforces that 4 km CRM resolution is too coarse to simulate such clouds and their response to climate change.

4. Implications for global cloud feedback uncertainty

The principal motivation for studies of cloud response to climate change using high-resolution models is to reduce (or at least better understand) uncertainty about global and regional cloud feedbacks and their potential interaction with rainfall and circulation trends. Unlike GCMs, LESs and CRMs explicitly simulate the turbulent circulations that form and interact with cloud systems, greatly reducing the complexity needed to represent moist processes including their subgrid variability. This does not guarantee more realistic results in all circumstances, but it does sidestep some of the most difficult GCM parametrization challenges, such as cumulus parametrization, interaction of cloud fraction, turbulence, microphysics, etc., allowing LES/CRM models to naturally simulate phenomena that have been long-standing challenges for GCMs, such as decoupled boundary layers, shallow cumulus convection, cold pools, and the Madden–Julian oscillation, and transitions between cloud regimes such as stratocumulus, shallow cumulus and deep cumulus. High-resolution models have limitations for climate studies, but given their complementary strengths, it would be reassuring if they give a view of cloud feedbacks that is consistent with the CMIP5 range of GCMs, and indeed that appears to be the case.

In table 1 and figure 5, we attempt to summarize the implications of LES/CRM studies discussed in this paper for cloud feedbacks, acknowledging that some of these studies use limited-area models and do not explicitly predict global feedbacks. Because the LES sensitivity studies are all idealized, e.g. by using steady forcings, they produce 'pure' low cloud types with SWCREs that can be much larger or smaller than climatologically observed in the most comparable real cloud regime, which inevitably includes a mixture of cloud types. Therefore, table 1 normalizes LES-implied SWCRE responses to be more representative of a corresponding real cloud regime by multiplying by the ratio of the annual-mean satellite-derived SWCRE to that of the model simulation. Since the LES studies are of low cloud regimes, their implied longwave cloud feedbacks are small and in some cases not documented, so they are omitted from table 1 and figure 5. Based on preliminary results from an intercomparison of five LESs using the same 'dCMIP3' forcings for the CGILS cases (PN Blossey 2015, personal communication), the quoted shortwave feedback strengths for the LES cases have an estimated intermodel spread of 50–150% of their tabulated values (but, reassuringly, all LESs agree on the sign of the feedback). In the two cumulus cases, the simulated SWCRE perturbations are particularly small and are likely to be sensitive to specification details.

In all cases, multi-day simulations are required, mandating computational domains generally smaller than 10×10 km. Larger LES domains can more realistically represent the observed mesoscale organization of these cloud regimes [68], and it is unknown how that might impact the simulated cloud response to a climate perturbation.

The LES cases are tightly controlled and focus on individual archetypical cloud regimes. Hence, it is not surprising that the simulated cloud feedbacks in these cases are more robust
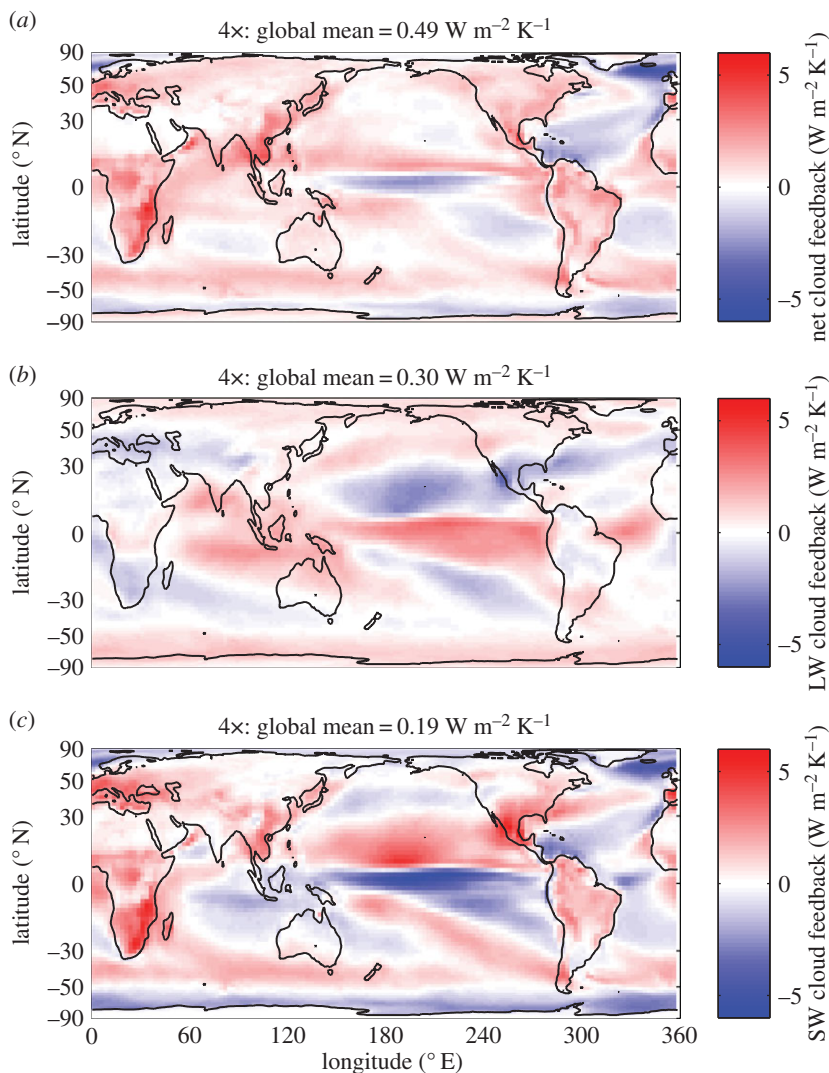
Figure 4. (a–c) Net cloud feedback from a superparametrized GCM coupled to a dynamical ocean, the SP-CESM4, diagnosed following [64] between years 100 and 150 of control and abrupt 4 × CO$_2$ simulations. Adapted from [61]. (Online version in colour.)

across models than global cloud feedbacks in GCMs and global high-resolution models that must simulate a wide assortment of cloud regimes. The main LES take-away message from figure 5 is that, overall, LESs predict stratocumulus cloud reduction and positive cloud feedback as the climate warms; with less certainty, they suggest that shallow cumulus may also slightly reduce, though it is fairly insensitive to warming.

   For other high-resolution model types, there are too few realizations to draw robust conclusions. The RCE simulations were on small domains, and larger domain RCE simulations are susceptible to convective aggregation [68,69], which may increase at warmer temperatures [70]. The RCE framework is arguably too idealized to address how large-scale convective organization changes in a warmer climate, but superparametrized simulations also show an amplified Madden–Julian oscillation over warmer SSTs [71]. The NICAM GCRM is better suited for this purpose, as it is becoming capable of sufficiently long simulations to study the temperature sensitivity of convective organization over the full range of realistic scales and with realistic geography. But one such model is not enough to draw robust conclusions given

Table 1. Cloud feedbacks simulated in various LES and cloud-resolving models. $C_{s,l}$ refer to shortwave and longwave cloud feedbacks. Italicized numbers refer to local cloud feedbacks; other estimates are global cloud feedbacks. For the LES cases, only local cloud shortwave feedback is estimated since marine boundary-layer clouds produce minimal longwave feedback. S_n, $n = 6, 11, 12$ refer to CGILS cases discussed in the text. The coefficients $\alpha_6 = 1.3$, $\alpha_{11} = 0.4$, $\alpha_{12} = 0.4$ are ratios of CERES satellite estimates of the annual mean SWCRE at the three NE Pacific CGILS locations ($-41, -64, -59$ W m^{-2}) to the simulated SWCRE in the corresponding LES control simulations ($-31, -168, -152$ W m^{-2}), and for these cases we take $\Delta T = 3$ K, the CMIP3 multi-model mean climate sensitivity. Blossey et al. [18] considered the cloud response to greenhouse warming in multi-day Lagrangian LESs of a northeast Pacific subtropical stratocumulus to cumulus transition over SSTs that increase downstream, based on a composite case introduced by Sandu & Stevens [65]. The tabulated estimates are an average of their P4CO2 perturbation with a climate locally warmed by 4 K and with quadrupled CO_2, and their dEIS perturbation with the free troposphere warmed by 4 K but the SST warmed by only 2 K; this averaged scenario is based on work by Qu et al. [66] and others that suggest significant EIS increases in the stratocumulus regions. In this case, the corresponding global temperature increase is estimated as $\Delta T_L = 5$ K. For the Lagrangian case, the LES control case has a SWCRE of 100 W m^{-2} compared with satellite observations that average approximately 50 W m^{-2} in annual mean along the simulated composite trajectory, so we take $\alpha_L = 0.5$. For all local models, the shortwave cloud feedback is calculated from the cloud radiative effect change by adding a masking correction of 1 W m^{-2} K^{-1} estimated from fig. 10 of [5] for the warm tropical ocean regions. For RCE, the longwave cloud feedback is assumed equal to the cloud radiative effect change by adding a masking correction of 1 W m^{-2} K^{-1} following estimates in [63]. The CMIP5 number and parenthesized range refer to multi-model range and total model spread in the total (shortwave plus longwave) cloud feedback.

| type	case	models	C_s	C_l	data given	calculation method	references
			(W m^{-2} K^{-1})				
LES							
Sc (mixed)	S12 dCMIP3	SAM	2.3	—	ΔCRE_s	$\alpha_{12} \Delta CRE_s / \Delta T$	[23]
Sc (decoupled)	S11 dCMIP3	SAM	2.0	—	ΔCRE_s	$\alpha_{11} \Delta CRE_s / \Delta T$	[23]
Cu (precip.)	S6 dCMIP3	SAM	1.3	—	ΔCRE_s	$\alpha_6 \Delta CRE_s / \Delta T$	[23]
Sc–Cu trans.	Sandu/GASS P4CO2 + dEIS	SAM	2.3	—	P4CO2 ΔCRE_s dEIS ΔCRE_s	$\alpha_L \Delta CRE_s / \Delta T_L$	[24]
Cu (non-prec.)	RICO-like $\Delta T = 8$ K	UCLA	0.3	—	$\Delta cc / cc = -14\%$;	$\Delta C_s = -15(\Delta cc/cc)$	[21]
CRM							
Rad.-Conv. Eq. ($\Delta x = 2$ km)	$\Delta SST = \pm 2$ K 60 × 60 km	Shutts	0.4	0.5	table 3	local $\Delta CRE_s / \Delta T$ local $\Delta CRE_l / \Delta T + 1$	[48]
global CRM ($\Delta x = 14$ km)	$\Delta SST = 2$ K	NICAM- CS4MYNN	1.4	1.5	ΔCRE_s (Fig. 1) ΔCI (Fig. 8)	$C_s \approx \Delta CRE_s / \Delta T + 0.2$ ISCCP simulator	[55]
Superparam. ($\Delta x = 4$ km)	$\Delta SST = 2$ K	SPCAM3	−0.8	0.7	ΔCRE_s ΔCRE_l	$C_s \approx \Delta CRE_s / \Delta T + 0.2$ $C_l \approx \Delta CRE_l / \Delta T + 0.65$	[62]
	abrupt 4×CO2	SPCCSM4	0.3	0.2	Fig. 6	ISCCP simulator	[61]
GCM							
	+1% CO2 yr^{-1}	CMIP3	0.35	0.35	Fig. 3	corrected ΔCRE	[67]
	abrupt 4 × CO2	CMIP5	0.7	(0.2–1.4)	Fig. 7.10	various	[2]
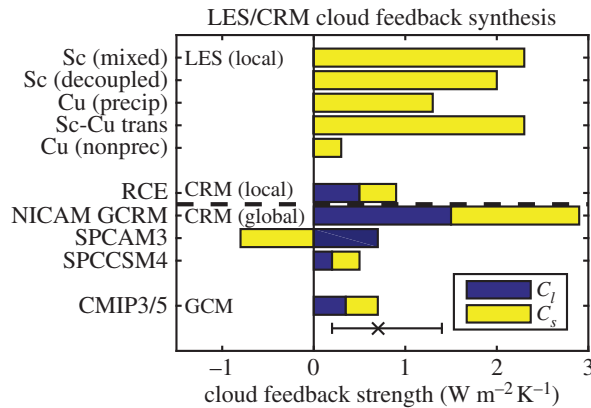
Figure 5. Synthesis of shortwave (light yellow) and longwave (dark blue) cloud feedbacks predicted by different types of LES and CRM simulations, based on table 1. LES and RCE values above the black dashed line are for the simulated regime; other values are global means. LES results (which are for boundary-layer clouds) do not show longwave feedbacks, which should in any case be small. The black cross and range below the lowest bar indicates the mean and range of the CMIP5 total (shortwave plus longwave) global cloud feedback. (Online version in colour.)

the uncertainties of microphysical, turbulent and surface parametrization that remain even in a GCRM. A future comparison of multiple GCRMs will be needed, as well as further observational evaluation of the realism of GCRMs in simulating multi-scale organization of deep convective cloud regimes. In any case, the diversity of global shortwave cloud feedbacks simulated by global high-resolution models suggests that 4 km resolution is inadequate to robustly simulate boundary-layer cloud regimes, at least until more advanced turbulence parametrizations have been deployed that can skilfully bridge the scale gap between 100 m wide boundary-layer updrafts and current GCRM grid resolutions.

From figure 5, we conclude that, compared with the CMIP5 GCMs, high-resolution global models do not systematically predict higher or lower global cloud feedbacks nor do they suggest a narrower feedback range. LESs do hint that cloud feedbacks may be more positive than the CMIP5 global mean in the subtropical marine stratocumulus regimes and their downstream transitions into trade cumulus, but more studies are needed to confirm that this conclusion is robust to simulation details. High-resolution models have been particularly useful in isolating observationally verifiable mechanisms of cloud feedback (e.g. FAT, enhanced low cloud mixing efficiency). Identification of robust positive feedback mechanisms has bolstered our confidence in the GCM and IPCC consensus that overall global cloud feedbacks are likely to be positive, and hence that ECS is more than 2 K and possibly as large as 4.5 K. In addition, LESs suggest that low cloud response can be regarded as a linear combination of responses to a few primary forcing agents such as changes in surface temperature, inversion strength, subsidence, radiative driving or wind speed [23] that operate on all time scales and can therefore be observationally calibrated based on daily to interannual variability and then extrapolated to infer regionally varying cloud responses to climate change [72]. In the next decade, computational and observational advances make the prospects for further insights from high-resolution modelling of cloud feedbacks bright, though the challenges to realizing this potential also loom large due to the diverse processes that regulate clouds around the world.

University), Stephan de Roode (TU Delft) and Bjorn Stevens (MPI Hamburg) for the use of high-resolution models as a benchmark for GCM cloud feedback studies helped CGILS get through early complications and achieve scientific impact.

References

1. Meehl GA *et al*. 2007 Global climate projections. In *Climate change 2007: the physical science basis* (eds S Solomon *et al*.), ch. 10. Cambridge, UK: Cambridge University Press.
2. Flato G *et al*. 2013 Evaluation of climate models. In *Climate change 2013: the physical science basis* (eds TF Stocker *et al*.), ch. 9. Cambridge, UK: Cambridge University Press.
3. Soden BJ, Held IM. 2006 An assessment of climate feedbacks in coupled ocean-atmosphere models. *J. Climate* **19**, 3354–3360. (doi:10.1175/JCLI3799.1)
4. Cess RD *et al*. 1989 Interpretation of cloud-climate feedback as produced by 14 atmospheric general circulation models. *Science* **245**, 513–516. (doi:10.1126/science.245.4917.513)
5. Soden BJ, Held IM, Colman R, Shell KM, Kiehl JT, Shields CA. 2008 Quantifying climate feedbacks using radiative kernels. *J. Climate* **21**, 3504–3520. (doi:10.1175/2007JCLI2110)
6. Ringer MA, Andrews T, Webb MJ. 2014 Global-mean radiative feedbacks and forcing in atmosphere-only and coupled atmosphere-ocean climate change experiments. *Geophys. Res. Lett.* **41**, 4035–4042. (doi:10.1002/2014GL060347)
7. Bony S, Dufresne J-L, Le Treut H, Morcrette J-J, Senior C. 2004 On dynamic and thermodynamic components of cloud changes. *Clim. Dyn.* **22**, 71–86. (doi:10.1007/s00382-003-0369-6)
8. Qu X, Hall A, Klein SA, Caldwell PM. 2014 On the spread of changes in marine low cloud cover in climate model simulations of the 21st century. *Clim. Dyn.* **42**, 2603–2626. (doi:10.1007/s00382-013-1945-z)
9. Sherwood SC, Bony S, Dufresne J-L. 2014 Spread in climate model sensitivity traced to atmospheric convective mixing. *Nature* **505**, 37–42. (doi:10.1038/nature12829)
10. Siebesma AP *et al*. 2003 A large-eddy simulation intercomparison study of shallow cumulus convection. *J. Atmos. Sci.* **60**, 1201–1219. (doi:10.1175/1520-0469(2003)60<1201:ALESIS>2.0.CO;2)
11. Bretherton CS *et al*. 1999 An intercomparison of radiatively-driven entrainment and turbulence in a smoke cloud, as simulated by different numerical models. *Quart. J. R. Meteorol. Soc.* **125**, 391–423. (doi:10.1002/qj.49712555402)
12. Stevens B *et al*. 2005 Evaluation of large-eddy simulations via observations of nocturnal marine stratocumulus. *Mon. Weather Rev.* **133**, 1443–1462. (doi:10.1175/MWR2930.1)
13. Ackerman AS *et al*. 2009 Large-eddy simulations of a drizzling, stratocumulus-topped marine boundary layer. *Mon. Weather Rev.* **137**, 1083–1110. (doi:10.1175/2008MWR2582.1)
14. VanZanten M *et al*. 2010 Controls on precipitation and cloudiness in simulations of trade-wind cumulus as observed during RICO. *J. Adv. Model. Earth Syst.* **3**, M04001. (doi:10.1029/2011MS000056)
15. Morrison H, Curry JA, Khvorostyanov VI. 2005 A new double-moment microphysics parameterization for application in cloud and climate models. *Part I: Description. J. Atmos. Sci.* **62**, 1665–1677. (doi:10.1175/JAS3446.1)
16. Kogan YL, Khairoutdinov MP, Lilly DK, Kogan ZN, Liu Q. 1995 Modeling of stratocumulus cloud layers in a large eddy simulation model with explicit microphysics. *J. Atmos. Sci.* **52**, 2923–2940. (doi:10.1175/1520-0469(1995)052<2923:MOSCLI>2.0.CO;2)
17. van der Dussen JJ *et al*. 2013 The GASS/EUCLIPSE model intercomparison of the stratocumulus transition as observed during ASTEX: LES results. *J. Adv. Model. Earth Syst.* **5**, 483–499. (doi:10.1002/jame.20033)
18. Blossey PN *et al*. 2013 Sensitivity of marine low clouds to an idealized climate change: the CGILS LES intercomparison. *J. Adv. Model. Earth Syst.* **5**, 234–258. (doi:10.1002/jame.20025)
19. Blossey PN, Bretherton CS, Wyant MC. 2009 Understanding subtropical low cloud response to a warmer climate in a superparameterized climate model. Part II: Column modeling with a cloud-resolving model. *J. Adv. Model. Earth Syst.* **1**, 8. (doi:10.3894/JAMES.2009.1.8)
20. Xu K-M, Cheng A, Zhang M. 2010 Cloud-resolving simulation of low-cloud feedback to an increase in sea-surface temperature. *J. Atmos. Sci.* **67**, 730–748. (doi:10.1175/2009JAS3239.1)

21. Rieck M, Nuijens L, Stevens B. 2012 Marine boundary-layer cloud feedbacks in a constant relative humidity atmosphere. *J. Atmos. Sci.* **69**, 2538–2550. (doi:10.1175/JAS-D-11-0203.1)

22. Zhang M *et al.* 2013 CGILS: Results from the first phase of an international project to understand the physical mechanisms of low cloud feedbacks in general circulation models. *J. Adv. Model. Earth Syst.* **5**, 826–842. (doi:10.1002/2013MS000246)

23. Bretherton CS, Blossey PN, Jones CR. 2013 Mechanisms of marine low cloud sensitivity to idealized climate perturbations: a single-LES exploration extending the CGILS cases. *J. Adv. Model. Earth Syst.* **5**, 316–337. (doi:10.1002/jame.20019)

24. Bretherton CS, Blossey PN. 2014 Low cloud reduction in a greenhouse-warmed climate: results from Lagrangian LES of a subtropical marine cloudiness transition. *J. Adv. Model. Earth Syst.* **6**, 91–114. (doi:10.1002/2013MS000250)

25. Dussen JJ, de Roode SR, Dal Gesso S, Siebesma AP. 2015 An LES model study of the influence of the free troposphere on the stratocumulus response to a climate perturbation. *J. Adv. Model. Earth Syst.* **7**, 670–691. (doi:10.1002/2014MS000380)

26. Klein SA, Hartmann DL. 1993 The seasonal cycle of low stratiform clouds. *J. Clim.* **6**, 1587–1606. (doi:10.1175/1520-0442(1993)006<1587:TSCOLS>2.0.CO;2)

27. Wood R, Bretherton CS. 2006 On the relationship between stratiform low cloud cover and lower tropospheric stability. *J. Clim.* **19**, 6425–6432. (doi:10.1175/JCLI3988.1)

28. Kamae Y, Watanabe M. 2012 On the robustness of tropospheric adjustment in CMIP5 models. *Geophys. Res. Lett.* **39**, L23808. (doi:10.1029/2012GL054275)

29. Myers TA, Norris JR. 2013 Observational evidence that enhanced free-tropospheric subsidence reduces marine boundary layer cloudiness. *J. Clim.* **26**, 7507–7524. (doi:10.1175/JCLI-D-12-00736.1)

30. Bony S, Dufresne JL. 2005 Marine boundary layer clouds at the heart of cloud feedback uncertainties in climate models. *Geophys. Res. Lett.* **32**, L20806. (doi:10.1029/2005GL023851)

31. Christensen MW, Carrio GG, Stephens GL, Cotton WR. 2013 Radiative impacts of free-tropospheric clouds on the properties of marine stratocumulus. *J. Atmos. Sci.* **70**, 3102–3118. (doi:10.1175/JAS-D-12-0287.1)

32. Kamae Y, Watanabe M. 2013 Tropospheric adjustment to increasing CO_2: its timescale and the role of land-sea contrast. *Clim. Dyn.* **41**, 3007–3024. (doi:10.1007/s00382-012-1555-1)

33. Nuijens L, Stevens B. 2012 The influence of wind speed on shallow marine cumulus convection. *J. Atmos. Sci.* **69**, 168–184. (doi:10.1175/JAS-D-11-02.1)

34. Wyant MC, Bretherton CS, Blossey PN. 2009 Understanding subtropical low cloud response to a warmer climate in a superparameterized climate model. Part I: Regime sorting and physical mechanisms. *J. Adv. Model. Earth Syst.* **1**, 7. (doi:10.3894/JAMES.2009.1.7)

35. Stevens B. 2007 On the growth of layers of non-precipitating cumulus convection. *J. Atmos. Sci.* **64**, 2916–2931. (doi:10.1175/JAS3983.1)

36. Nuijens L, Serikov I, Hirsch L, Lonitz K, Stevens B. 2014 The distribution and variability of low-level cloud in the North Atlantic trades. *Q. J. R. Meteorol. Soc.* **140**, 2364–2374. (doi:10.1002/qj.2307)

37. Kuang Z, Bretherton CS. 2006 A mass flux scheme view of a high-resolution simulation of transition from shallow to deep cumulus convection. *J. Atmos. Sci.* **63**, 1895–1909. (doi:10.1175/JAS3723.1)

38. Andrews T, Gregory JM, Webb MJ, Taylor KE. 2012 Forcing, feedbacks and climate sensitivity in CMIP5 coupled atmosphere-ocean climate models. *Geophys. Res. Lett.* **39**, L09712. (doi:10.1029/2012GL051607)

39. Zelinka MD, Klein SA, Taylor KE, Andrews T, Webb MJ, Gregory JM, Forster PM. 2013 Contributions of different cloud types to feedbacks and rapid adjustments in CMIP5. *J. Clim.* **26**, 5007–5027. (doi:10.1175/JCLI-D-12-00555.1)

40. Vial J, DuFresne J-L, Bony S. 2013 On the interpretation of inter-model spread in CMIP5 climate sensitivity estimates. *Clim. Dyn.* **41**, 3339–3362. (doi:10.1007/s00382-013-1725-9)

41. Zhang M, Bretherton CS. 2008 Mechanisms of low cloud climate feedback in idealized single-column simulations with the Community Atmospheric Model (CAM3). *J. Clim.* **21**, 4859–4878. (doi:10.1175/2008JCLI2237.1)

42. Nuijens L, Medeiros B, Sandu I, Ahlgrimm M. 2015 The behavior of trade wind cloudiness in observations and models: the major cloud components and their variability. *J. Adv. Model. Earth Syst.* **7**, 600–616. (doi:10.1002/2014MS000390)

18

rsta.royalsocietypublishing.org   *Phil. Trans. R. Soc. A* **373**: 20140415

43. Brient F, Schneider T, Tan Z, Bony S. Submitted. Shallowness of tropical low clouds as a predictor of climate models' response to warming.

44. Stainforth DA *et al*. 2005 Uncertainty in predictions of the climate response to rising levels of greenhouse gases. *Nature* **433**, 403–406. (doi:10.1038/nature03301)

45. Gettelman A, Kay JE, Shell KM. 2012 The evolution of climate sensitivity and climate feedbacks in the Community Atmosphere Model. *J. Clim.* **25**, 1453–1469. (doi:10.1175/JCLI-D-11-00197.1)

46. Zhao M. 2014 An investigation of the connections among convection, clouds, and climate sensitivity in a global climate model. *J. Clim.* **27**, 1845–1861. (doi:10.1175/JCLI-D-13-00145.1)

47. Webb MJ *et al*. 2015 The impact of parametrized convection on cloud feedback. *Phil. Trans. R. Soc. A* **373**, 20140414. (doi:10.1098/rsta.2014.0414)

48. Tompkins AM, Craig GC. 1999 Sensitivity of tropical convection to sea surface temperature in the absence of large-scale flow. *J. Clim.* **12**, 462–476. (doi:10.1175/1520-0442(1999)012<0462:SOTCTS>2.0.CO;2)

49. Kuang Z, Hartmann DL. 2007 Testing the fixed anvil temperature hypothesis in a cloud-resolving model. *J. Clim.* **20**, 2051–2057. (doi:10.1175/JCLI4124.1)

50. Hartmann DL, Larson K. 2002 An important constraint on tropical cloud-climate feedback. *Geophys. Res. Lett.* **29**, 1951–1954. (doi:10.1029/2002GL015835)

51. Zelinka MD, Hartmann DL. 2010 Why is longwave cloud feedback positive? *J. Geophys. Res.* **115**, D16117. (doi:10.1029/2010JD013817)

52. Lindzen RS, Chou M-D, Hou AY. 2001 Does the Earth have an adaptive infrared iris? *Bull. Amer. Meteorol. Soc.* **82**, 417–432. (doi:10.1175/1520-0477(2001)082<0417:DTEHAA>2.3.CO;2)

53. Miura H, Tomita H, Nasuno T, Iga S, Satoh M. 2005 A climate sensitivity test using a global cloud-resolving model under an aquaplanet condition. *Geophys. Res. Lett.* **32**, L19717. (doi:10.1029/2005GL023672)

54. Satoh M, Iga S, Tomita H, Tsushima Y, Noda AT. 2012 Response of upper clouds in global warming experiments obtained using a global nonhydrostatic model with explicit cloud processes. *J. Clim.* **25**, 2178–2191. (doi:10.1175/JCLI-D-11-00152.1)

55. Tsushima Y, Iga S, Tomita H, Satoh M, Noda AT, Webb MJ. 2014 High cloud increase in a perturbed SST experiment with a global nonhydrostatic model including explicit convective processes. *J. Adv. Model. Earth Syst.* **6**, 571–585. (doi:10.1002/2013MS000301)

56. Grabowski W. 2001 Coupling cloud processes with the large-scale dynamics using the cloud-resolving convection parameterization (CRCP). *J. Atmos. Sci.* **58**, 978–997. (doi:10.1175/1520-0469(2001)058<0978:CCPWTL>2.0.CO;2)

57. Khairoutdinov MF, Randall DA. 2001 A cloud-resolving model as a cloud parameterization in the NCAR Community Climate System Model: preliminary results. *Geophys. Res. Lett.* **28**, 3617–3620. (doi:10.1029/2001GL013552)

58. Khairoutdinov MF, DeMott C, Randall DA. 2005 Simulation of the atmospheric general circulation using a cloud-resolving model as a super-parameterization of physical processes. *J. Atmos. Sci.* **62**, 2136–2154. (doi:10.1175/JAS3453.1)

59. Stan C, Khairoutdinov M, DeMott CA, Krishnamuthy V, Straus DM, Randall DA, Kinter III JL, Shukla J. 2010 An ocean-atmosphere climate simulation with an embedded cloud resolving model. *Geophys. Res. Lett.* **27**, L01702. (doi:10.1029/2009GL040822)

60. Stan C, Xu L. 2014 Climate simulations and projections with the super-parameterized CCSM4. *Env. Model. Software* **60**, 1234–1152. (doi:10.1016/j.envsoft.2014.06.013)

61. Bretherton CS, Blossey PN, Stan C. 2014 Cloud feedbacks on greenhouse warming in the superparameterized climate model SP-CCSM4. *J. Adv. Model. Earth Syst.* **6**, 1185–1204. (doi:10.1002/2014MS000355)

62. Wyant MC, Khairoutdinov M, Bretherton CS. 2006 Climate sensitivity and cloud response of a GCM with a superparameterization. *Geophys. Res. Lett.* **33**, L06714. (doi:10.1029/2005GL025464)

63. Wyant MC, Bretherton CS, Blossey PN, Khairoutdinov M. 2012 Fast cloud adjustment to increasing CO_2 in a superparameterized climate model. *J. Adv. Model Earth Syst.* **4**, M05001. (doi:10.1029/2011MS000092)

64. Zelinka MD, Klein SA, Hartmann DL. 2012 Computing and partitioning cloud feedbacks using cloud property histograms. Part I: cloud radiative kernels. *J. Clim.* **25**, 3715–3735. (doi:10.1175/JCLI-D-11-00248.1)

65. Sandu I, Stevens B. 2011 On the factors modulating the stratocumulus to cumulus transitions. *J. Atmos. Sci.* **68**, 1865–1881. (doi:10.1175/2011jas3614.1)

66. Qu X, Hall A, Kein SA, Caldwell PM. 2014 The strength of the tropical inversion and its response to climate change in 18 CMIP5 models. *Clim. Dyn.* **45**, 375–396. (doi:10.1007/s00382-014-2441-9)

67. Soden BJ, Vecchi GA. 2011 The vertical distribution of cloud feedback in coupled ocean-atmosphere models. *Geophys. Res. Lett.* **38**, L12704. (doi:10.1029/2011GL046732)

68. Tompkins AM. 2001 Organization of tropical convection in low vertical wind shears: the role of water vapor. *J. Atmos. Sci.* **58**, 529–545. (doi:10.1175/1520-0469(2001)058<0529:OOTCIL>2.0.CO;2)

69. Bretherton CS, Blossey PN, Khairoutdinov M. 2005 An energy-balance analysis of deep convective self-aggregation above uniform SST. *J. Atmos. Sci.* **62**, 4273–4292. (doi:10.1175/JAS3614.1)

70. Khairoutdinov MF, Emanuel KA. 2013 Rotating radiative-convective equilibrium simulated by a cloud-resolving model. *J. Adv. Model. Earth Syst.* **5**, 816–825. (doi:10.1002/2013MS000253)

71. Arnold N, Kuang Z, Tziperman E. 2013 Enhanced MJO-like variability at high SST. *J. Clim.* **26**, 988–1001. (doi:10.1175/JCLI-D-12-00272.1)

72. Myers TA, Norris JR. 2015 On the relationships between subtropical clouds and meteorology in observations and CMIP3 and CMIP5 models. *J. Clim.* **28**, 2945–2967. (doi:10.1175/JCLI-D-14-00475.1)

19

rsta.royalsocietypublishing.org *Phil. Trans. R. Soc. A* **373**: 2014 0415